Journal of Physics and Chemistry of Solids 191 (2024) 111984

Contents lists available at ScienceDirect

Journal of Physics and Chemistry of Solids

journal homepage: www.elsevier.com/locate/jpcs

Investigation of the performance and properties of ZnO/GO double-layer supercapacitor

Handan Büyükkürkçü [a], Ali Durmuş [b], Hakan Çolak [c], Rifat Kurban [d], Ertuğrul Şahmetlioğlu [e], Ercan Karaköse [e,*]

[a] Department of Graduate Education Institute, Electrical-Electronics Engineering, Kayseri University, 38280, Talas, Kayseri, Turkey
[b] Department of Electrical and Electronics Engineering, Engineering & Architecture and Design Faculty, Kayseri University, 38280, Talas, Kayseri, Turkey
[c] Department of Chemistry, Faculty of Science, Çankırı Karatekin University, 18100, Çankırı, Turkey
[d] Department of Computer Engineering, Engineering Faculty, Abdullah Gul University, Kayseri, Turkey
[e] Department of Natural Sciences, Engineering & Architecture and Design Faculty, Kayseri University, 38280, Talas, Kayseri, Turkey

ARTICLE INFO

Keywords:
Supercapacitor
Graphene oxide
Electrode
Zinc oxide

ABSTRACT

Composite electrode material was formed by mixing reduced graphene oxide (rGO) and zinc oxide (ZnO) compound, using the Hummers and green synthesis methods, respectively. Of rGO powder, 10 g was mixed with 10%, 20% and 30% ZnO, and composite electrodes were obtained by using 10% binder. The energy storage performance and structural characteristics of the supercapacitor were evaluated by analyzing the capacitance values of the synthesized electrodes. The structural characterization of ZnO/rGO composites was performed using X-ray diffraction and field-emission scanning electron microscopy. The electrochemical properties of the ZnO/GO electrodes were analyzed by cyclic voltammetry, electrochemical impedance and galvanostatic charge–discharge tests. The specific capacitance value of electrodes increased as zinc content increased in the ZnO/rGO composite material used to produce electrodes. The maximum specific capacitance values were measured at 5 mV/s scanning rate as 194.23 (rGO), 366.81 (10% ZnO), 383.18 (20% ZnO) and 410.48 F/g (30% ZnO). In conclusion, the use of composite material formed by the combination of ZnO nanoparticles obtained by green synthesis method from orange peel and graphene oxide increased the electrochemical efficiency of the supercapacitor.

1. Introduction

With the spread and development of technology, the need for energy has increased. In order to meet the increasing demand for energy, renewable (convertible) energy sources along with new-generation energy storage techniques, are needed [1,2]. The preferred power sources in new-generation energy storage systems are dielectric capacitors, lithium-ion batteries and supercapacitors. While dielectric capacitors are preferred for micro-sized and short-term electronics, lithium-ion batteries are preferred for medium-term electricity storage devices, with supercapacitors falling between these two electronic technologies. Although capacitors and supercapacitors have similar working principles, their energy storage rates differ. While energy is stored in the capacitor by the accumulation of electrical charges on the plates used, energy storage in supercapacitors occurs through the accumulation of charges on the electrode and electrolyte separator [3,4]. Supercapacitors are used in power supply and storage, either instead of batteries or in combination with batteries, where there is a sudden power requirement. There are three basic categories that make frequent use of supercapacitors. The first category is transportation vehicles – by providing the initial movement in vehicles such as electric bicycles, automobiles, trams, buses and trains, supercapacitors extend the life of the battery or engine, significantly reducing fuel and maintenance costs of the vehicles. The second category is uninterrupted power supplies such as UPS – supercapacitors are used in uninterrupted power supplies of buildings and industrial plants. In case of any interruption or sudden voltage changes in power supplies, supercapacitors protect the system by providing backup power to electronic cards. The third category is electronic products – supercapacitors are used in flashes, speakers, keyboard keys, cameras, various electronic devices, electric motors, electroshock devices, image recorders, TV satellite receivers, and radio station memory backup elements [4–7]. Electrochemical double-layer

* Corresponding author.
E-mail addresses: ercankarakose@gmail.com, ekarakose@kayseri.edu.tr (E. Karaköse).

https://doi.org/10.1016/j.jpcs.2024.111984
Received 31 October 2023; Received in revised form 7 March 2024; Accepted 8 March 2024
Available online 11 March 2024

capacitors are capacitors that store energy by trapping electrical charge in the electrical double-layer, which forms through the accumulation of ions on the interface with electrodes of a large porous carbon structure [8]. The electrodes are separated from each other by a separator. Each electrode–electrolyte interface functions as a separate capacitor [9]. The two electrode materials and electrolyte molecules form an "electrical double layer" at their interface. This stored energy is very efficient compared to other types of capacitors as it charges and discharges quickly [10,11]. Especially in recent years, different groups of substances have been added to carbon to improve the electrical capacitance of electrochemical double-layer supercapacitors. Vegetable-based fibers such as agricultural wastes, fruit seeds, wood or fossil-based additives such as coal, lignite and petroleum are preferred [12–14]. In today's world, minimizing damage to the environment in energy production is crucial for preventing environmental problems. Nanostructured zinc oxide (ZnO) is an n-type semiconductor, which is an environmentally friendly metal oxide due to its wide band gap of 3.37 eV, high electrochemical stability, high exciton binding energy of 60 MeV and non-toxic properties. In addition, "green synthesis" (GS) methods are based on using environmentally friendly reagents and do not pose any environmental risks during synthesis [15–17]. In this study, for the first time, ZnO nanoparticles were obtained from orange peel using the GS method, considering its environmentally friendliness and simplicity. The reasons for preferring orange peel in GS can be summarized as follows: (a) Turkey accounts for 4% of world orange production and is seventh in the world in production; (b) utilization of orange peel, which is considered waste; and (c) presence of phytochemicals, flavonoids, antioxidants, vitamins A, B and C, as well as trace amounts of elements Cu, Mg and Ca in orange peel. The ZnO/rGO composite electrodes were formed by doping reduced graphene oxide (rGO) powder obtained using Hummer's method and ZnO nanoparticles in specific proportions. The structural properties of these composite electrodes were characterized, and their performance analyzed.

2. Experimental procedure

2.1. Production of graphene oxide using Hummer's technique

Graphene oxide (GO) was synthesized using Hummer's method. Graphite powder (10 g of different purity), 250 g of sulfuric acid and phosphoric acid (in a 9:1 vol ratio) were slowly added to a 1000-ml beaker and stirred gently until thoroughly combined [18]. Potassium permanganate (8 g) was gradually added with continuous stirring for 1 h. The temperature was raised to 60 °C and kept under agitation for 12 h. To prevent the reaction, 700 ml of ice-cold water and 1 ml of 30% H_2O_2 were slowly added to dilute the substance. A color change from brown to yellow was observed. The resulting product was washed with a 10% HCl solution and deionized water until pH neutralization. Then, the obtained product was washed with ethanol and dried at 60 °C in a hot-air oven for 12 h. Dark brown GO powder was obtained. Of this powder, 10 g was stirred with 100 ml of pure water for 30 min and annealed at 950 °C for 12 h. The resulting suspension solution changed from dark brown to dark black.

2.2. Synthesis of rGO

For the reduction process, 600 ml of deionized water was added to 2 g of powdered GO, mixed for 8 h at 35 °C and processed in an ultrasonic bath for 2 h. Of hydrazine hydrate (H_6N_2O), 60 ml was added to the mixture and stirred at 95 °C for 8 h with a magnetic stirrer. The mixture was left to cool at room temperature and first washed with acetone and then with non-ionized water and filtered on a filter [19]. The obtained material was dried at room temperature and powdered rGO was obtained.

2.3. Green synthesis ZnO nanoparticle production using orange peel

Fresh orange peel (10 g) was used for plant extracts. The shells were washed with distilled water and boiled in 100 ml of distilled water at 100 °C for 60 min and allowed to cool. The plant extract was collected by filtration on filter paper. Of the extract, 50 ml was mixed with 5 g of Zn $(NO_3)_2$ and heat treated at 100 °C until it gelled [20]. The gel mixture was annealed at 400 °C for 120 min and the material was ground in an agate mortar to obtain ZnO nanoparticles. The production step of ZnO nanoparticles from orange peel is shown in Fig. 1.

2.4. Production of ZnO/rGO nanocomposite electrodes

Electrodes were synthesized by hydrothermal method by incorporating ZnO and rGO materials at specified rates. The ZnO/rGO composite electrode materials were created as follows. To obtain a homogeneous suspension, 10 g of rGO was mixed in 10 ml of ethanol under ultrasonication for 3 h at 25 C. Of zinc nitrate hexahydrate [Zn $(NO_3)_2{\cdot}6H_2O$, ZnO source], 1 g and hexamethylenetetramine ($C_6H_{12}N_4$) were dissolved in 1 ml of ethanol. Subsequently, this solution was added to the previous solution. Then, a *N*-methyl pyrrolidone binder was added to the mixture. A hydrothermal process was carried out at 95 °C for 4 h to produce a ZnO/rGO composite electrode material. This was then dried at room temperature. The doped zinc ratios varied (20 wt % and 30 wt % ZnO) and were added into the GO powder using the same applications, and new composite electrodes were formed. Table 1 contains the names and abbreviations of the synthesized samples.

2.5. Characterization analysis techniques

The energy storage performance and characterization of the structural properties of a supercapacitor with varying capacitance values of the synthesized electrodes were analyzed. Structural characterization of ZnO/rGO composites was performed using X-ray diffraction (XRD), Raman spectroscopy, X-ray photoelectron spectroscopy (XPS) and field scanning electron microscopy (FE-SEM). The electrochemical properties of the produced ZnO/rGO electrodes were analyzed by cyclic voltammetry (CV), electrochemical impedance and galvanostatic charge–discharge (GCD) tests. The crystallographic structures of the fabricated materials were characterized using XRD (Rikagu XRD) equipped with a Cu-Kα radiation emitter. A Raman spectrophotometer (WITec alpha 300 M + micro-Raman system, Germany) equipped with a 532-nm laser source was used to acquire the materials' Raman spectra. The microstructure of the samples was observed with a FE-SEM (Zeiss Gemini 600). The electrochemical performance of the prepared ZnO-doped electrodes was evaluated in a three-electrode configuration using CV, GCD and electrochemical impedance spectroscopy in 1 M KOH aqueous electrolyte. For comparison, the CV of rGO and ZnO/rGO electrodes with a thickness of 800 nm was measured at the same scanning rate.

3. Results and discussion

3.1. FE-SEM analysis

The FE-SEM analysis results are crucial in determining morphological characteristics of materials. In our study, the surface structures of rGO and ZnO/rGO composite (ZnGO, 2ZnGO and 3ZnGO) electrodes were compared. Each electrode was analyzed using FE-SEM images at 20,000 × magnification. Images of the rGO electrode are given in Fig. 2a and of ZnGO, 2ZnGO and 3ZnGO electrodes in Fig. 2b–d, respectively. The rGO surface shows distributed homogeneous nanoparticles and irregular particles of different sizes (Fig. 2a).

With the addition of ZnO to rGO for ZnGO, nanorod structures are shown in the structure by FE-SEM (Fig. 2b). The FE-SEM image for 2ZnGO shows ZnO attached to the surface of the rGO material, the ZnO

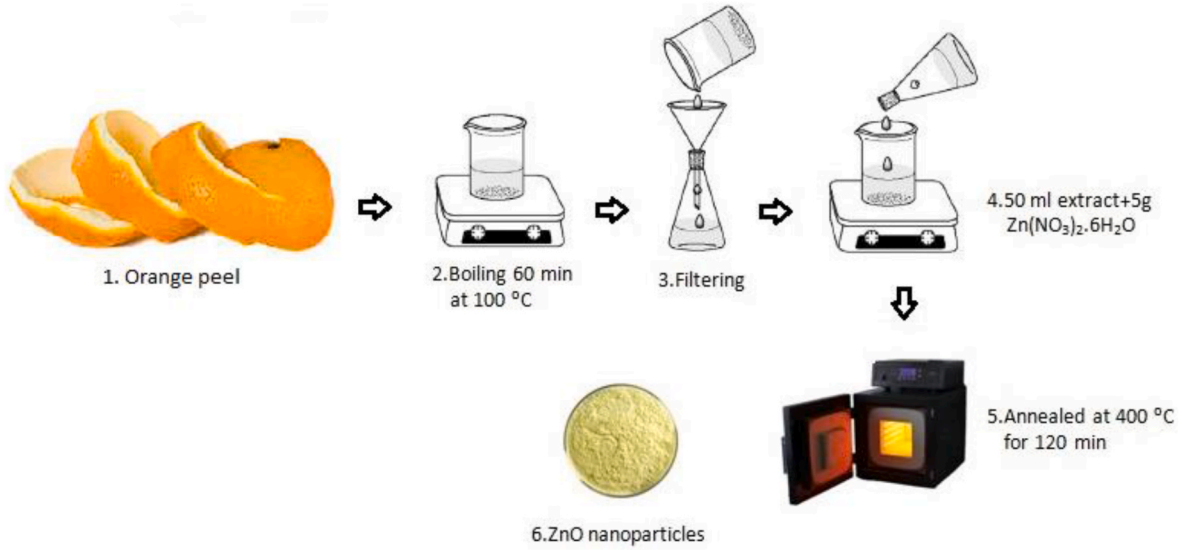

Fig. 1. Schematic description of ZnO nanoparticle synthesis from orange peel [21].

Table 1
Sample names and abbreviations.

Sample name	Sample abbreviation
Reduced graphene oxide	rGO
Reduced graphene oxide with 10 wt %ZnO doped	ZnGO
Reduced graphene oxide with 20 wt %ZnO doped	2ZnGO
Reduced graphene oxide with 30 wt %ZnO doped	3ZnGO

layer is visible as a white-colored layer and ZnO nanorods are evident (Fig. 2c). The FE-SEM for 3ZnGO shows ZnO nanorods attached to the surface and partially white ZnO structures (Fig. 2d).

The cross-sectional structures of ZnGO, 2ZnGO, and 3ZnGO electrodes are shown in Fig. 3. The FE-SEM images show that ZnO nanoparticles form complexes with GO particles. Close examination of the structure shows ZnO nanorods. Furthermore, density of ZnO nanorods increases with increased amount of ZnO.

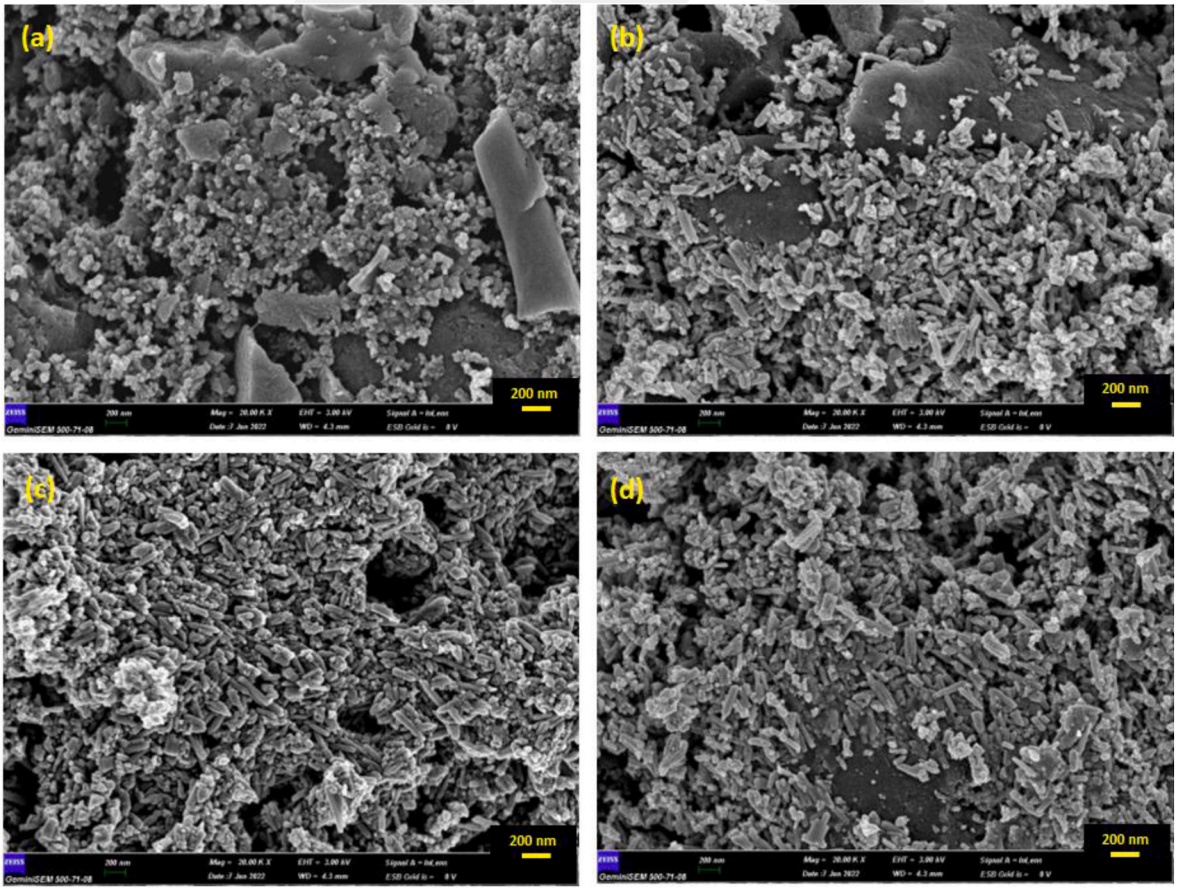

Fig. 2. FE-SEM images of ZnO/rGO: (a) rGO, (b) ZnGO (c) 2ZnGO and (d) 3ZnGO.

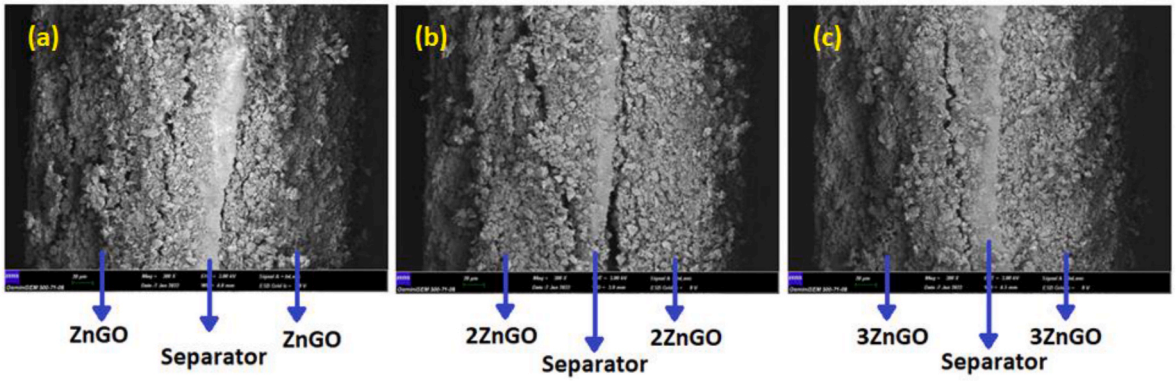

Fig. 3. The structure of (a) ZnGO, (b) 2ZnGO and (c) 3ZnGO electrode capacitors.

3.2. XRD, Raman and XPS analysis

In XRD analysis, crystal structures were analyzed in the range of 10–90°. The XRD peaks of the synthesized electrodes are shown in Fig. 4. Fig. 4a shows the XRD result for rGO. The diffraction peak of RGO is at 26°, which corresponds to the diffraction peak of the (002) plane diffraction of graphite carbon. The peaks of both ZnO and rGO are shown in Fig. 4b–d. The 2θ diffraction angles of the wurtzite structure of ZnO (JCPDS 396–1451) are located at 32.81°, 33.48°, 36.41°, 46.57°, 55.43°, 61.88°, 65.46°, 67.55°, 74.47°, 76,92° and 80.26°, corresponding to the (100), (002), (101), (102), (110), (103), (200), (112), (004), (202), and (104) planes. Similar peaks have been detected in other studies [22–24]. The XRD peaks around 26° and 44° correspond to the (002) and (100) planes of rGO, while all other peaks correspond to the ZnO wurtzite structure (Fig. 4b–d). The coexistence of peaks belonging to ZnO and rGO reveals that ZnO nanoparticles are doped into rGO.

Raman spectroscopy is a unique method used to determine the molecular properties and bonding states of nanostructured carbon-based materials [25,26]. Fig. 5 shows the Raman spectroscopy of rGO and ZnO/rGO nanoparticles. Characteristic D and G bands for rGO, ZnGO and 3ZnGO samples are shown at 1356 and 1586 cm^{-1}, respectively. The D and G bands provide information about the molecular structural properties of a graphene sample. The D band indicates dislocations and structural defects in graphene, while the G band reflects the sp^2 symmetry of the C–C bond. The G band is highly sensitive to stress, doping and interactions, and shifts very slightly with introduction of ZnO into the structure [27]. This suggests a possible interaction between GO and ZnO.

The surface composition and chemical properties of materials can be examined using XPS analysis. This analysis method interacts with the electrons on the material surface using X-rays and measures their kinetic

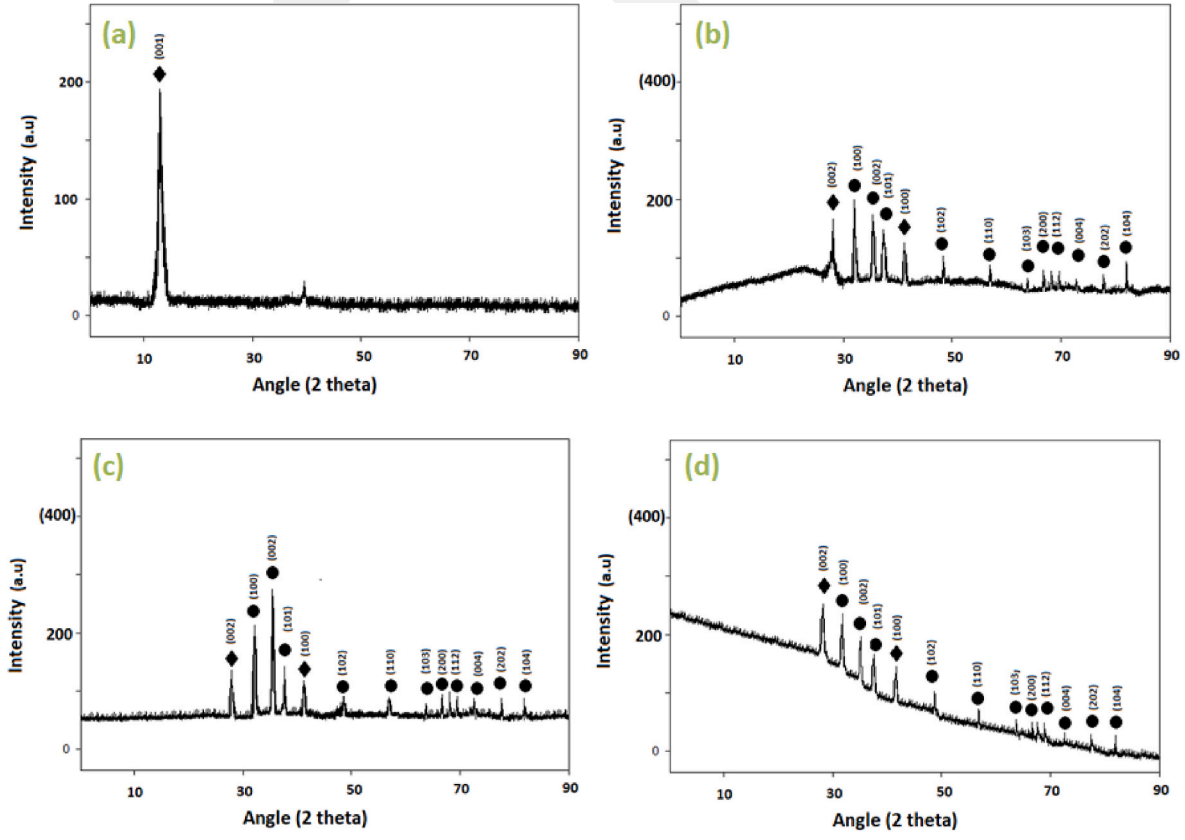

Fig. 4. XRD analysis of GO and ZnO/rGO: (a) rGO, (b) ZnGO (c) 2ZnGO and (d) 3ZnGO.

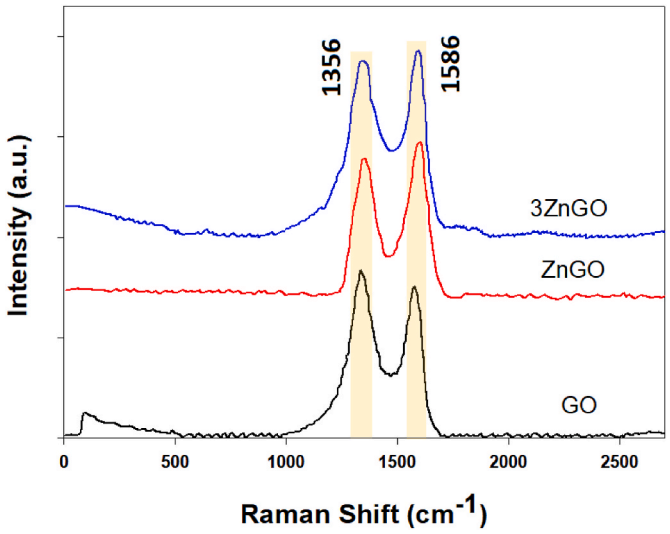

Fig. 5. Raman spectra of GO and ZnO/rGO composites.

energies. This provides information about the surface composition and chemical bonds of materials. It is particularly preferred for determining the chemical structure on the surface of organic and inorganic compounds. The XPS analysis was performed to analyze the surface composition and chemical properties of rGO, ZnGO, 2ZnGO and 3ZnGO composite electrodes (Fig. 6).

Fig. 6a shows only two peaks in the scanning spectra of rGO, corresponding to the C (1s) and O (1s) orbitals with binding energies of 285.2 and 531.4 eV, respectively. New peaks are evident for the ZnGO, 2ZnGO and 3ZnGO electrodes (Fig. 6b–d, respectively). These peaks belong to Zn (3 d), Zn (3p), and Zn (3s) with binding energies of 8.20, 90.42 and 135.44 eV, respectively [28]. The C1s spectra of rGO and 3ZnGO are shown in Fig. 7a and b, and the 2p spectrum of 3ZnGO in Fig. 7c. The C1s has three bond peaks: C–C (283.5 eV), C–O (285.8 eV) and C═O (288.8 eV) (Fig. 7a) [29]. Additionally, in the C (1s) spectrum of the 3ZnGO composite, there is a distinctive peak at 280.4 eV (Fig. 7b), corresponding to the Zn–C bond [30]. Peaks at 282.7 and 285.6 eV are identified as C–C bonds [30,31]. Furthermore, a peak at 287.9 eV may be attributed to the C–O–Zn bond, formed between the O–H group on rGO and Zn–O – a relationship also supported by FTIR analysis [30,32]. The measured energy difference between the Zn $2p_{3/2}$ (2021.8 eV) and Zn $2p_{1/2}$ (1043.92 eV) orbitals is 22.8 eV (Fig. 7c), indicating that the Zn atom is in the form of Zn^{2+} ions [33].

3.3. Electrochemical analysis

The changes in capacitance values of rGO, ZnO, 2ZnGO and 3ZnGO composite electrodes at scanning speeds of 5, 10, 20, 50 and 70 mV/s are given in Fig. 8. The specific capacitance and charge storage values of composite electrodes made of rGO, ZnGO, 2ZnGO and 3ZnGO, measured at the lowest scanning rate (5 mV/s), have values of 194.23, 366.81, 383.18 and 410.48 F/g, respectively. The results show the highest capacitance value for the 3ZnGO composite electrode (i.e. 30% ZnO addition). The capacitance of the 3ZnGO electrode is higher than the ZnGO and 2ZnGO electrodes produced with 20% and 10% ZnO materials, respectively. The increased ratio of ZnO nanoparticles in the

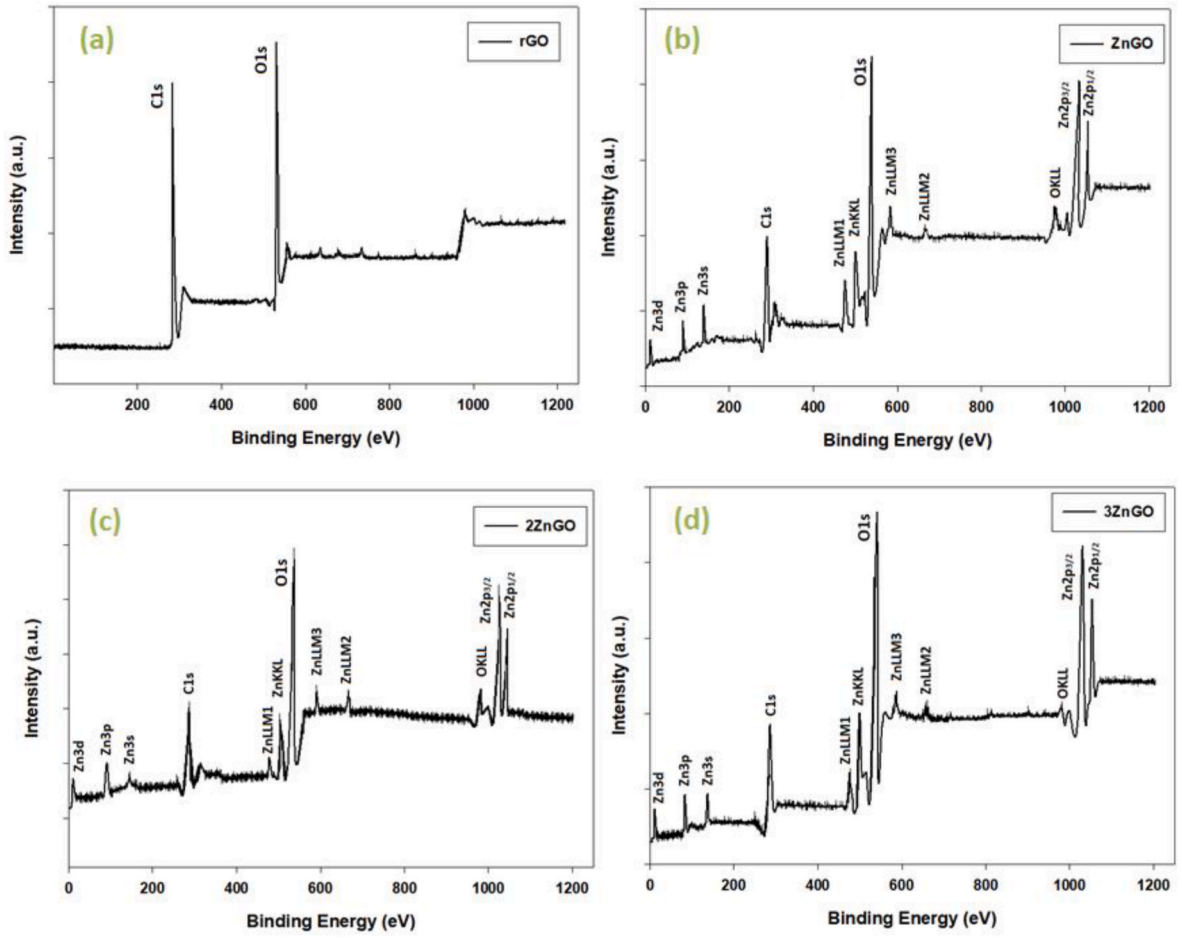

Fig. 6. XPS spectra of ZnO/rGO: (a) rGO, (b) ZnGO (c) 2ZnGO and (d) 3ZnGO.

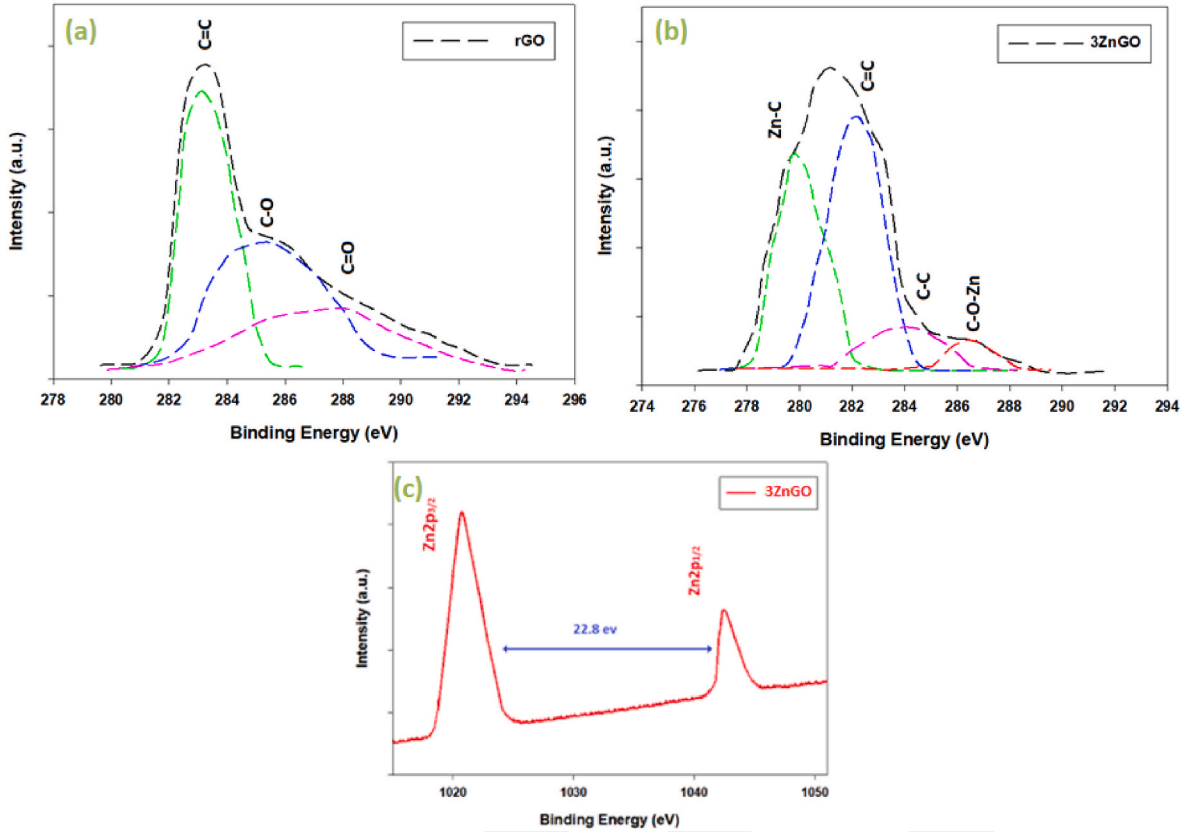

Fig. 7. XPS spectra of 3ZnGO composite: (a) rGO C1s, (b) 3ZnGO C1s, (c) 3ZnGO 2p.

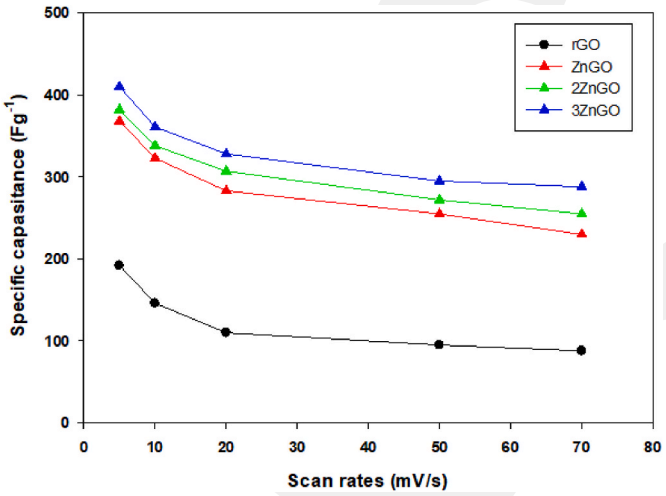

Fig. 8. Specific capacitance of ZnO/rGO composites at various scanning rates.

mixture facilitates the retention of electrons in the oxygen groups in graphene and increases specific capacitance value [34].

The use of CV helps understanding of the thermodynamic and kinetic properties of a chemical reaction and also to determine the reaction mechanism. Fig. 9a–d shows the CV measurements of rGO and composite ZnO/GO electrodes at scan rates of 5, 10, 20, 50 and 70 mV/s in the fixed potential range of −0.5 to +0.5 V. Peak current densities increase as the scan rate increases. The current–potential curve of 3ZnGO electrodes has the highest cyclic volume of current and potential, which supports better performance of the 3ZnGO composite electrode with a 30% increase in specific capacitance.

The specific capacitance values of the electrodes are measured in electrochemical CV analyses using 1000 cycles. The percentage decrease in specific capacitance values after 1000 cycles is similar for all electrodes (Fig. 10). The electrode 3ZnGO synthesized shows less decrease in specific capacitance percentage compared to other composites (ZnGO and 2ZnGO) after 1000 cycles, indicating a longer lifespan of the 3ZnGO electrode than other composite electrodes. The Nyquist curves showing the electrochemical impedance values of rGO, ZnO, 2ZnGO and 3ZnGO samples are shown in Table 2 and Fig. 11. The Nyquist curve shows the frequency response of an electronic circuit and is used to examine the dynamic behavior of the circuit and also provide information about the circuit's mutual interactions. Nyquist curves are used to evaluate features such as power loss and power efficiency of the circuit. The intersection of the Nyquist curve with the x (real) axis gives the electron's intrinsic resistance (ESR). The equivalent series resistance, also known as intrinsic resistance, includes the resistance of the electrolyte solution used and the resistance of the electrode and current-carrying elements [35]. The measured ESR values of rGO, ZnO, 2ZnGO and 3ZnGO are approximately 10.5, 8.7, 6.9 and 4.3 Ω, respectively. The 3ZnGO capacitor exhibits a smaller internal resistance compared to the other capacitors (Table 2). This small ESR value is ascribed to the enhanced accessibility of electrolyte ions to the surface of graphene sheets and ZnO crystals facilitated by the ZnO/graphene hybrid [36].

Fig. 12 shows the charge–discharge curves for rGO, ZnGO, 2ZnGO and 3ZnGO electrodes. During charge–discharge, Zn^{+} ions from the electrolyte contribute to the charge storage of ZnGO, 2ZnGO and 3ZnGO composite electrodes. The GCD curves of rGO and composite ZnGO, 2ZnGO and 3ZnGO electrodes synthesized by adding different percentages of ZnO are measured in the range of 0–0.8 V at current densities of 0.1, 0.3 and 0.5 A/g. The charge–discharge times decrease as current density increases, and total charge–discharge times increase with increased ZnO percentage [37].

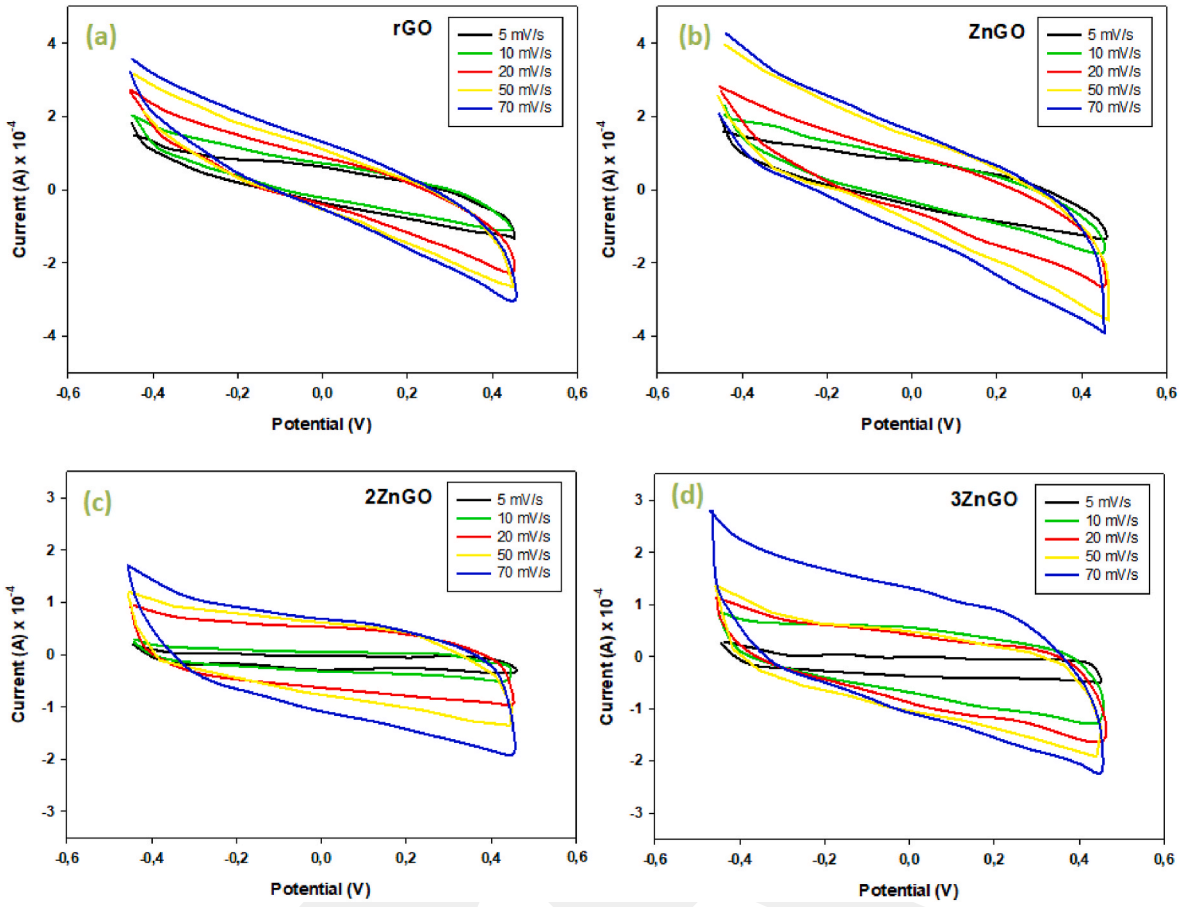

Fig. 9. Charge–discharge curves of ZnO/rGO composites with different current densities.

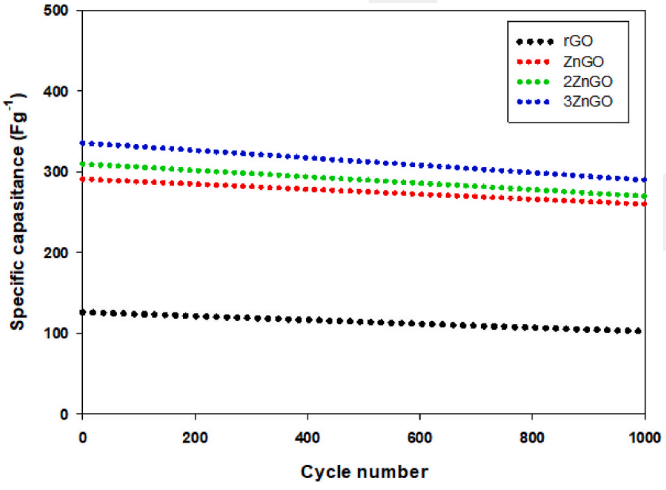

Fig. 10. Specific capacitance depending on the number of cycles of ZnO/rGO composites.

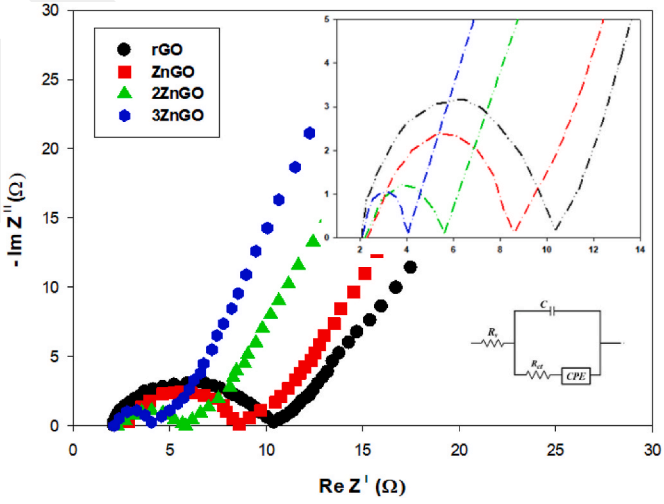

Fig. 11. Nyquist curves of rGO and ZnO/rGO composite electrodes.

Table 2
Measured ESR values of electrodes.

Samples	ESR (Ω)
rGO	10.5
ZnGO	8.7
2ZnGO	6.9
3ZnGO	4.3

4. Conclusions

In this study, Zn/rGO composite electrodes were formed by incorporating different percentages of ZnO nanoparticles produced via the GS method into the rGO material. The FE-SEM surface images showed that ZnO nanoparticles were included in the nanorod-shaped composite. Electrochemical analysis of ZnO/rGO composite electrodes showed that the 3ZnGO electrode had the highest specific capacitance value (410.48 F/g) at the lowest scan rate (5 mV/s). The capacitance property of the

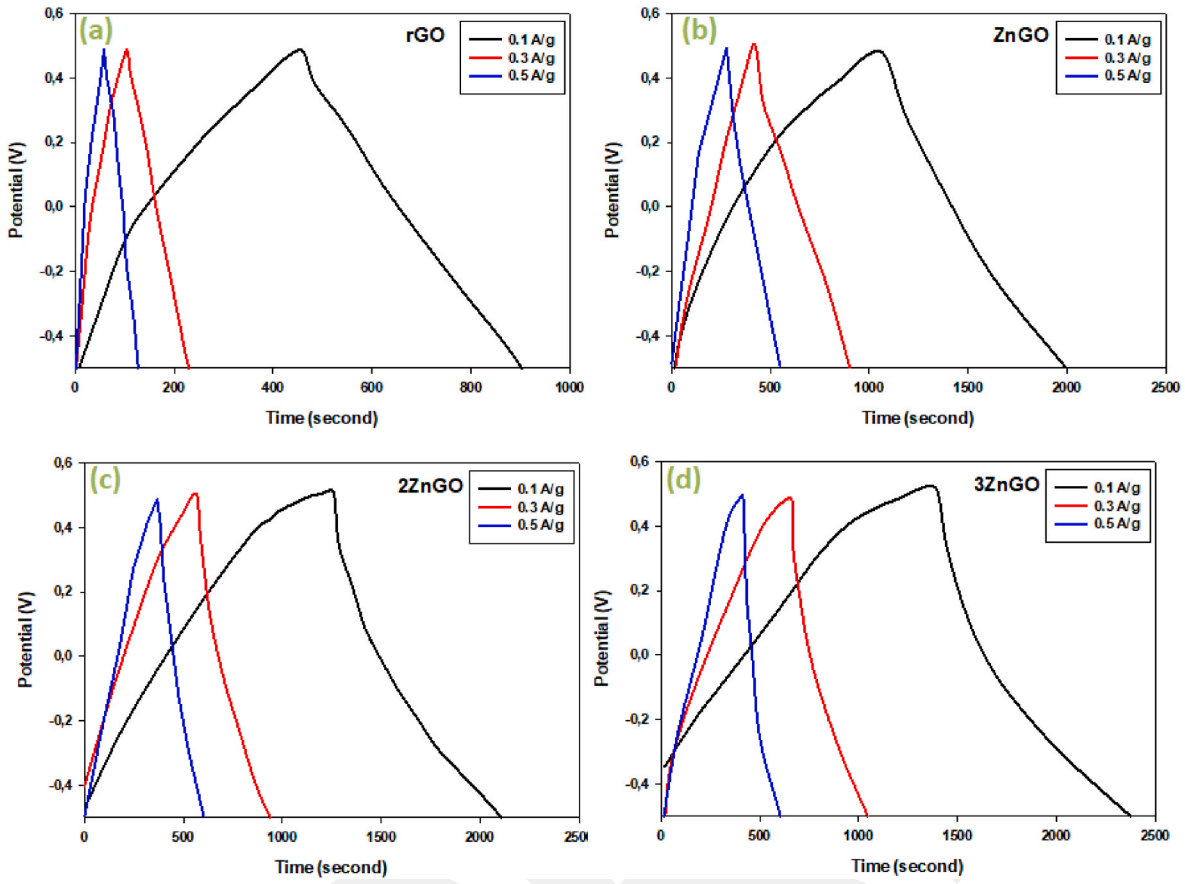

Fig. 12. Charge–discharge graph of ZnO/rGO composites: (a) rGO, (b) ZnGO (c) 2ZnGO and (d) 3ZnGO.

3ZnGO electrode produced with a ZnO ratio of 30% was higher than for the ZnGO and 2ZnGO electrodes produced with 10% and 20% ZnO materials, respectively. The increased ratio of ZnO nanoparticles in the mixture facilitated the retention of electrons in the oxygen groups of graphene. At the end of 1000 cycles of the electrodes, the reduction rates in specific capacitance were very close to each other as percentages and the rate of change was low. Additionally, the GCD test showed that charge–discharge times of the electrodes varied proportionally with the zinc percentage.

CRediT authorship contribution statement

Handan Büyükkürkçü: Writing – original draft, Methodology, Investigation, Formal analysis. **Ali Durmuş:** Writing – original draft, Resources, Project administration, Funding acquisition. **Hakan Çolak:** Validation, Investigation, Conceptualization. **Rifat Kurban:** Writing – review & editing, Data curation. **Ertuğrul Şahmetlioğlu:** Writing – review & editing, Supervision, Funding acquisition, Data curation. **Ercan Karaköse:** Writing – original draft, Methodology, Investigation, Formal analysis, Data curation, Conceptualization.

Declaration of competing interest

The authors declare that they have no known competing financial interests or personal relationships that could have appeared to influence the work reported in this paper.

Data availability

Data will be made available on request.

Acknowledgements

This research was financially supported by the Kayseri University Scientific Research Projects Unit (Project BAP, FYL-2022-1059) and the Turkish Scientific and Technical Research Institute (TUBITAK) (Project 115F045).

References

[1] G. Yu, X. Xie, L. Pan, Z. Bao, Y. Cui, Hybrid nanostructured materials for high-performance electrochemical capacitors, Nano Energy 2 (2013) 213–234.
[2] M.I. Rafiq, T. Farid, J. Zhou, A. Ali, J. Tang, W. Tang, Carbonized wood-supported hollow $NiCo_2S_4$ eccentric spheres for high-performance hybrid supercapacitors, J. Alloys Compd. 811 (2019) 151858.
[3] S. Yetiman, F.K. Dokan, M.S. Onses, E. Yılmaz, E. Sahmetlioglu, Hybrid electrodes composed of graphitic carbon nitride and zeolitic imidazolate framework-67 for supercapacitor applications, Int. J. Energy Res. 46 (2022) 22730–22743.
[4] Ü. Alver, A. Tanrıverdi, Ö. Akgül, Hydrothermal preparation of ZnO electrodes synthesized from different precursors for electrochemical supercapacitors, Synth. Met. 211 (2016) 30–34.
[5] D. Feng, T. Lei, M.R. Lukatskaya, J. Park, Z. Huang, M. Lee, Z. Bao, Robust and conductive two-dimensional metal–organic frameworks with exceptionally high volumetric and areal capacitance, Nat. Energy 3 (2018) 30–36.
[6] H. Peçenek, F.K. Dokan, M.S. Onses, E. Yılmaz, E. Sahmetlioglu, Outstanding supercapacitor performance with intertwined flower-like NiO/MnO_2/CNT electrodes, Mater. Res. Bull. 149 (2022) 111745.
[7] S. Yetiman, H. Peçenek, F.K. Dokan, M.S. Onses, E. Yılmaz, E. Sahmetlioglu, Microwave-assisted fabrication of high-performance supercapacitors based on electrodes composed of cobalt oxide decorated with reduced graphene oxide and carbon dots, J. Energy Storage 49 (2022) 104103.
[8] A.G. Pandolfo, A.F. Hollenkamp, Carbon properties and their role in supercapacitors, J. Power Sources 157 (2006) 11–27.
[9] R. Kötz, M. Carlen, Principles and applications of electrochemical capacitors, Electrochim. Acta 45 (2000) 2483–2498.
[10] J.R. Miller, P. Simon, Electrochemical capacitors for energy management, Science 321 (2008) 651–652.
[11] P. Sharma, T.S. Bhatti, A review on electrochemical double-layer capacitors, Energy Convers. Manag. 51 (2010) 2901–2912.

[12] J.I. Hayashi, A. Kazehaya, K. Muroyama, A.P. Watkinson, Preparation of activated carbon from lignin by chemical activation, Carbon 38 (2000) 1873–1878.
[13] E. Yagmur, M. Ozmak, Z. Aktas, A novel method for production of activated carbon from waste tea by chemical activation with microwave energy, Fuel 87 (2008) 3278–3285.
[14] I. Gurten, M. Ozmak, E. Yagmur, Z. Aktas, Preparation and characterisation of activated carbon from waste tea using K_2CO_3, Biomass Bioenergy 37 (2012) 73–81.
[15] A. Gour, N.K. Jain, Advances in green synthesis of nanoparticles, Artif. Cells, Nanomed. Biotechnol. 47 (2019) 844–851.
[16] S.K. Srikar, D.D. Giri, D.B. Pal, P.K. Mishra, S.N. Upadhyay, Green synthesis of silver nanoparticles: a review, Green Sustain. Chem. 6 (2016) 34–56.
[17] H. Reinsch, "Green" synthesis of metal-organic frameworks, Eur. J. Inorg. Chem. 2016 (2016) 4290–4299.
[18] H. Yu, B. Zhang, C. Bulin, R. Li, R. Xing, High-efficient synthesis of graphene oxide based on improved hummers method, Sci. Rep. 6 (2016) 36143.
[19] C.K. Chua, M. Pumera, Chemical reduction of graphene oxide: a synthetic chemistry viewpoint, Chem. Soc. Rev. 43 (2014) 291–312.
[20] H. Çolak, E. Karaköse, Green synthesis and characterization of nanostructured ZnO thin films using Citrus aurantifolia (lemon) peel extract by spin-coating method, J. Alloys Compd. 690 (2017) 658–662.
[21] E. Karaköse, H. Çolak, F. Duman, Green synthesis and antimicrobial activity of ZnO nanostructures *Punica granatum* shell extract, Green Process. Synth. 6 (2017) 317–323.
[22] Y. Haldoraia, W. Voitb, J.-J. Shim, Nano ZnO@reduced graphene oxide composite for high performance supercapacitor: green synthesis in supercritical fluid, Electrochim. Acta 120 (2014) 65–72.
[23] J. Liu, X. Li, L. Dai, Water-assisted growth of aligned carbon nanotube-ZnO heterojunctions arrays, Adv. Mater. 18 (2006) 1740.
[24] O. Akhavan, Graphene nanomesh by ZnO nanorod photocatalysts, ACS Nano 4 (2012) 4174.
[25] R. Kumar, R.K. Singh, A.R. Vaz, R. Savu, S.A. Moshkalev, Self-assembled and one-step synthesis of interconnected 3D network of Fe_3O_4/reduced graphene oxide nanosheets hybrid for high-performance supercapacitor electrode, ACS Appl. Mater. Interfaces 9 (2017) 8880–8890.
[26] S. Meti, M.R. Rahman, M.I. Ahmad, K.U. Bhat, Chemical free synthesis of graphene oxide in the preparation of reduced graphene oxide-zinc oxide nanocomposite with improved photocatalytic properties, Appl. Surf. Sci. 451 (2018) 67–75.
[27] A. Ghosh, M. Miah, C. Majumder, S. Bag, D. Chakravorty, S.K. Saha, Synthesis of multilayered structure of nano-dimensional silica glass/reduced graphene oxide for advanced electrochemical applications, Nanoscale 10 (2018) 5539–5549.
[28] J. Liu, S. Li, B. Zhang, Y. Xiao, Y. Gao, Q. Yang, Y. Wang, G. Lu, Ultrasensitive and low detection limit of nitrogen dioxide gas sensor based on flower-like ZnO hierarchical nanostructure modified by reduced graphene oxide, Sensor. Actuator. B Chem. 249 (2017) 715–724.
[29] N.A. Devi, S. Nongthombam, S. Sinha, R. Bhujel, S. Rai, W.I. Singh, P. Dasgupta, B. P. Swain, Investigation of chemical bonding and supercapacitivity properties of Fe_3O_4-rGO nanocomposites for supercapacitor applications, Diam. Relat. Mater. 104 (2020) 107756.
[30] D. Yang, A. Velamakanni, G. Bozoklu, S. Park, M. Stoller, R.D. Piner, S. Stankovich, Chemical analysis of graphene oxide films after heat and chemical treatments by X-ray photoelectron and Micro-Raman spectroscopy, Carbon 47 (2009) 145–152.
[31] S. Salehi, M. Molaei, M. Karimipour, Mo-rich rGO–2H–$MoSe_2$ nanocomposites with novel crystal growth plane of (106) for high hydrogen evolution reaction activity, Mater. Sci. Semicond. Process. 142 (2022) 106475.
[32] S. Lu, H. Wang, J. Zhou, X. Wu, W. Qin, Atomic layer deposition of ZnO on carbon black as nanostructured anode materials for high-performance lithium-ion batteries, Nanoscale 9 (2017) 1184–1192.
[33] L. Jing, Z. Xu, X. Sun, J. Shang, W. Cai, The surface properties and photocatalytic activities of ZnO ultrafine particles, Appl. Surf. Sci. 180 (2001) 308–314.
[34] S. Nagarani, G. Sasikala, M. Yuvaraj, R.D. Kumar, S. Balachandran, M. Kumar, ZnO-CuO nanoparticles enameled on reduced graphene nanosheets as electrode materials for supercapacitors applications, J. Energy Storage 52 (2022) 104969.
[35] J. Zhang, L.B. Kong, J.J. Cai, Y.C. Luo, L. Kang, Nanoflake-like cobalt hydroxide/ordered mesoporous carbon composite for electrochemical capacitors, J. Solid State Electrochem. 14 (2010) 2065–2075.
[36] E. Samuel, P.U. Londhe, B. Joshi, M.W. Kim, K. Kim, S.S. Yoon, Electrosprayed graphene decorated with ZnO nanoparticles for supercapacitors, J. Alloys Compd. 741 (2018) 781–791.
[37] M. Miah, T.K. Mondal, A. Ghosh, S.K. Saha, Study of highly porous ZnO nanospheres embedded reduced graphene oxide for high performance supercapacitor application, Electrochim. Acta 354 (2020) 136675.